

# Maximizing solar photovoltaic energy efficiency: MPPT techniques investigation based on shading effects



Ana-Maria Badea <sup>a</sup>, Doina Manaila-Maximean <sup>a,b</sup>, Laurentiu Fara <sup>a,b,\*</sup>, Dan Craciunescu <sup>a</sup>

<sup>a</sup> National University of Science and Technology "Politehnica" Bucharest, Department of Physics, 313 Spl. Independentei, 060042 Bucharest, Romania

<sup>b</sup> Academy of Romanian Scientists, 3 Ilfov Str., RO-050094 Bucharest, Romania

## ARTICLE INFO

### Keywords:

PV Panels  
Solar cells  
Simulation  
Shading behavior Optimization  
Power output  
Energy efficiency

## ABSTRACT

This article presents a comprehensive study focused on understanding and optimizing the behavior of a photovoltaic (PV) generator. The study explores Maximum Power Point Tracking (MPPT), a critical technique used to optimize the energy output of a PV generator by dynamically adjusting under varying conditions of solar irradiance and temperature, ensuring that the PV generator operates at its most efficient level. By also accounting for shading effects, which can significantly impact energy production and overall performance, this research includes a detailed analysis of the shading effects on the illuminated area based on optimization-MPPT algorithms. Advanced modeling and simulation techniques are employed, with a particular emphasis on the Levenberg-Marquardt method for parameter estimation. This method is used to fit mathematical models to experimental PV generator data and extract relevant parameters. Additionally, the study leverages the "Curve Fitting Toolbox" method in MATLAB to fit mathematical models for experimental I-V and P-V data. The investigation utilizes an industrial polycrystalline silicon PV module and compares simulated results with experimental data. One significant aspect of the analysis is the examination of partial shading's impact on the PV generator. The results highlighted that partial shading poses a substantial challenge to the PV system, leading to a notable reduction in power output. The study presents various techniques for Maximum Power Point Tracking (MPPT) and analyzes their capabilities and performance metrics. The research methodology involves a combination of simulated and experimental data to understand how PV panels behave under different shading conditions. Furthermore, the study proposes an optimized configuration and advanced MPPT algorithms to enhance system performance in the presence of partial shading. The optimized setup not only increases power output but also enhances overall system efficiency and reliability by mitigating issues such as shading-induced hotspots and potential panel failures. The findings and strategies outlined in this study could be adapted and applied to various types of PV modules.

## 1. Introduction

As a result of different inducement initiatives and specific market circumstances in many European countries and globally, photovoltaic (PV) systems have risen as a key solution for residential housing and other independent applications [1,2,3]. This strategy brings to the forefront novel and vital concerns regarding the effectiveness,

dependability, and security of PV systems, whether they operate independently (standalone) or are integrated with the electrical grid [4,5]. Due to the continued decrease of the world's traditional energy sources, PV systems play a growing part in the mix of energy used to generate modern electric power. The key benefits of PV power systems include: (1) the absence of moving components; (2) the generation of negligible noise; (3) the minimal to no maintenance requisites and an

**Abbreviations:** PV, Photovoltaic; MPPT, Maximum Power Point Tracking; I-V, Current-Voltage characteristic; P-V, Power-Voltage characteristic; MPP, Maximum Power Point; P&O, Perturb & Observe; MP&O, Modified Perturb and Observe; IC, Incremental Conductance; RCC, Ripple Correlation Control; SCC, Short Circuit Current; OCV, Open Circuit Voltage; PSO, Particle Swarm Optimization; GWO, Grey Wolf Optimization; ACO, Ant Colony Optimization; ABC, Artificial Bee Colony; GN, Gauss Newton; FLC, Fuzzy Logic Controller; ANN, Artificial Neural Network; SMC, Sliding Mode Control; DISMC, Double Integral Sliding Mode Control; FPSO, Fuzzy Particle Swarm Optimization; ANFIS, Adaptive Neuro Fuzzy Interface System; FLC, Fuzzy Logic Controllers; TCT, Total Cross-Tied; SP, Series-Parallel; FCM, Fuzzy C-Mean; STC, Standard test condition; ANFIS, Adaptive Neuro Fuzzy Inference System; CS, Cuckoo Search.

\* Corresponding author.

E-mail address: [lfara@renerg.pub.ro](mailto:lfara@renerg.pub.ro) (L. Fara).

<https://doi.org/10.1016/j.solener.2024.113082>

Received 28 August 2024; Received in revised form 26 October 2024; Accepted 5 November 2024

Available online 21 November 2024

0038-092X/© 2024 The Author(s). Published by Elsevier Ltd on behalf of International Solar Energy Society. This is an open access article under the CC BY-NC-ND license (<http://creativecommons.org/licenses/by-nc-nd/4.0/>).

environmentally benign nature; (4) the renewable essence; (5) the high adaptability and dependability; (6) the suitability for installation in nearly any geographical location [6]. Critical facets of electricity generation, particularly its reliability and steadiness, exert substantial influence over the escalating demand for dependable electricity supply, thereby enhancing consumer safety [7,8]. Nonetheless, electricity production derived from renewable sources introduces challenges concerning harmonization with the prevailing electrical grid. A prominent challenge within PV systems revolves around power storage, constituting an important facet for enhancing performance in solar-powered communal setups [9,10]. Prior research has yielded design approaches for distributed and shared batteries; nevertheless, these existing methodologies hinge on aggregated community energy disparities [11,12]. While this approach may avert excessive battery sizing, it could precipitate a distinct issue, specifically substantial electricity losses during the transmission process, attributable to extended power transmission distances [13]. A notable research gap in the analysis of diverse algorithm applications related to optimizing the operation of PV systems, considering their performance, balance, and robustness under various shading conditions, is addressed in this study centered on Maximum Power Point Tracking (MPPT) and partial shading [14,15,16]. The findings obtained from this research could have implications for the application of other algorithms in optimizing various standalone or grid-integrated PV systems [17].

In order to obtain higher performance and commercialization of PV systems, it is essential to carry out individual analyses for each type of application, examining in detail their operational integration in specific contexts [18,19].

The operational optimization of PV systems depends on the refinement of MPPT techniques, that allow to be used for improved electrical performance of PV systems even under fluctuating operating conditions, largely influenced by meteorological factors but also by mechanical ones (e.g., dirt degree) [20,21].

The significant contribution of this paper revolves around the optimized enhancement of a PV system through: (1) investigation and implementation that involves a progressive approach employing series-parallel evaluation to examine shading effects on the studied PV generator (panel); (2) the precise operation of a PV system via numerical modeling to investigate the consequences of temperature and solar

irradiance on PV device performance, as well as its response to shading conditions [22,23]. This study's structure is built upon an enhanced numerical simulation model, implemented in MATLAB Simulink, directly leading to performance improvements in the PV generator.

Another goal addressed by this study is the accuracy and complexity of the investigation, which encompasses a broad spectrum in terms of information flow and outcomes. This is particularly notable given the scarcity of comprehensive practices in specialized literature. In the literature, there are mainly 4 categories of MPPT techniques applied to the PV systems.

These methods are designed to track MPP with high accuracy under dynamic and changing weather conditions. They have a very high capability to track the MPP efficiently. These techniques also involve high complexity in control circuits and extensive data handling for pre-training the system. To furnish a structured overview of these MPPT techniques, Fig. 1 presents the main classification of MPPT techniques, providing a good understanding for identifying the MPPT methods in the scientific literature [24,25].

## 2. Advancement of photovoltaic technology

### 2.1. State of the Art

In the realm of PV research and scientific exploration, the development of comprehensive models entails a meticulous consideration of input parameters that collectively shape the accuracy, reliability, and applicability of the model's outcomes. These input parameters, often referred to as input sizes or variables, serve as the bedrock upon which the predictive power of the model is built. The accurate representation of these parameters is paramount to crafting models that offer insights into the intricate behavior of PV systems under diverse operational conditions.

According to experts, individuals who own PV systems might experience a reduction of up to 30 % in potential energy production due to shading. Surprisingly, this isn't solely due to complete shading of a solar panel. Even if only 20 % of the panel's surface is shaded, the output power can decrease by as much as 50 %, as indicated by certain reports and research within the field. The main reason for this lies in the interconnection of solar cells within an array [26,27,28].

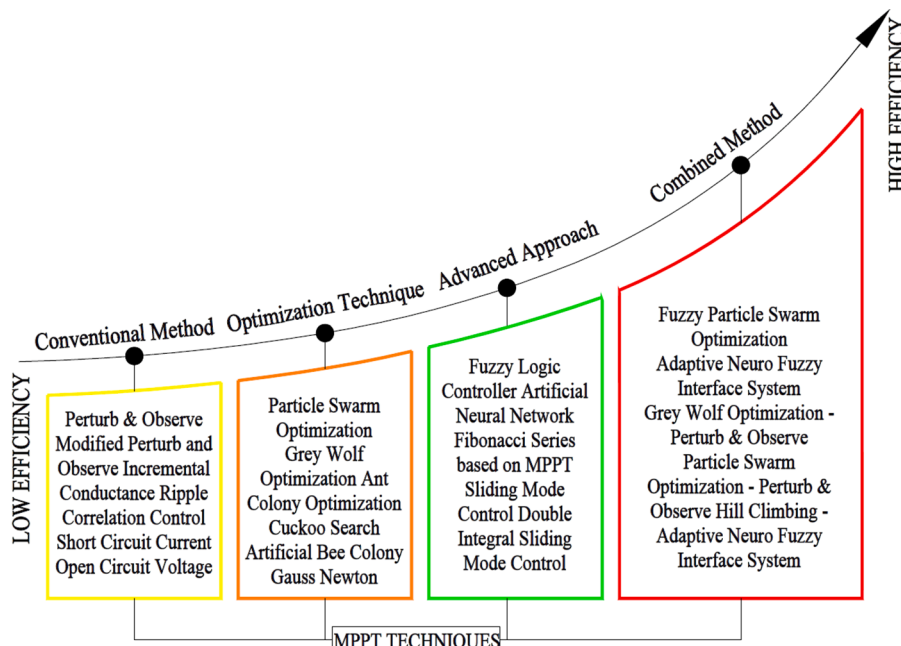


Fig. 1. Main classification of MPPT techniques.

Shading effects occur when certain sections of a PV system receive unequal solar irradiance due to obstructions [29,30]. In such scenarios, cells exposed to lower irradiance levels may actually absorb power instead of generating it. To mitigate this, bypass diodes are integrated to lessen the impact of shading and safeguard the panels [31]. PV arrays are often equipped with one or two diodes, usually positioned every 10 cells in a PV panel (adjusted based on the number of cells in a PV panel). By configuring the PV array in specific structure, the influence of shading on the whole PV system can be studied. To comprehensively evaluate and understand the behavior of PV panels, an effective approach involves the use of a MPPT system based on specialized algorithms such as FLC, P&O, BC or IC [32,33,34]. Commonly, solar cell arrays are linked in PV panels through a fusion of series – parallel connections known as “strings.” When shadowing occurs, the losses propagate throughout the entire string of cells. To prevent total failure, bypass diodes are typically employed [35,36]. These diodes redirect current away from damaged or inefficient cells. However, even with these measures, while the entire array might not fail simultaneously, the energy harvested from the cells is diminished. This leads to a reduction in the string’s voltage, consequently lowering the energy efficiency of the PV device [37,38].

A panel subjected to shading within a string can markedly diminish its output power. However, the output power of a parallel string is unaffected by the shading of another string. Consequently, an effective solution involves segregating shaded panels into distinct strings (parallel – series), which maximizes the overall output power of the PV array [39,40]. In practical terms, arranging shaded panels receiving shade from specific sources (like parapets) into one set of strings, while grouping unshaded panels into separate, parallel strings, can optimize power production. Determining the impact of shading on a PV panel demands a theoretically intricate approach, involving numerical modeling and simulation of the electrical parameters of the PV array [41,42].

An alternative strategy to enhance partial shade efficiency involves implementing an optimized controller [43,44]. This device adjusts output I-V to sustain maximum power without affecting other PV array performance. It is required to study algorithms for optimizing the MPP with techniques like Fuzzy Logic Controllers (FLC) being pertinent [45,46].

This approach facilitates efficient modeling and simulation of PV panel behavior while enabling adjustment of panel operation. Concurrently, an optimization strategy based on MPP tracking algorithms guarantees output power optimization accuracy, motivating ongoing research to refine these models and enhance PV system efficiency [47,48,49].

To illustrate, in a scenario where a shaded panel generates electricity at a reduced current level, a controller optimizer (utilizing established MPPT techniques) would elevate the output current to match unshaded panels while simultaneously lowering the output voltage by the same degree. This allows the shaded panel to contribute electricity without hindering the output of other panels [50]. For a deeper understanding of the shading impact, the present article schematically depicts the effect on PV cells and the associated implications for output power, along with potential optimization opportunities [51].

## 2.2. Literature review: Basic concepts and availability

In the specialized literature, topics concerning partial shading and the optimization of PV systems through MPPT techniques have garnered significant attention, engaging numerous researchers in the field. Some noteworthy contributions include: 1) Viorel Badescu introduced a straightforward constrained optimization approach, where the aim is to enhance electrical output power while adhering to current–voltage characteristics and energy balance within a series–parallel PV panel [35]. The research underscored the pronounced impact of latitude and climate on PV panel design, revealing that panels optimized for warmer

climates possess more solar cells in series and fewer solar cell strings compared to colder climates. Moreover, the optimal configuration of PV panels is intricately linked to the quality of the PV cells. 2) J. Vandana conducted a comprehensive study on the effects of shading patterns and intensity on Fully Cross-Tied (FCT) PV array configurations through advanced numerical simulations [16]. Also, their investigation encompassed three standard PV array setups utilizing series–parallel (SP) connections. 3) Similarly, H. Rezk, et al. examined methods to enhance efficiency and reduce investment costs in PV systems by employing a symmetrical approach [23]. Their research integrates mathematical and engineering principles to develop a balanced PV model, utilizing series–parallel circuit theory, piecewise functions, and MATLAB/Simulink simulations at an advanced level. 4) S. Chidurala, et al. proposed a minimalist approach to modeling the performance of solar panels under shading using the shading ratio. By integrating shadow area and opacity into the PV cell model, the authors aimed to provide a clearer understanding of PV system operation under shaded conditions. Furthermore, the analysis of shading ratios, coupled with image processing, offers valuable insights for evaluating and predicting the I-V behavior and MPPs of shaded PV panels. This approach is also applicable for monitoring operational PV installations [34]. 5) Carlos Robles Algarín et al. underscored the necessity of MPPT techniques and demonstrated their effectiveness in optimizing energy production across various climatic conditions [62].

They introduced an FLC based on MPPT controller, demonstrating its superiority and precision through simulation and numerical modeling. 6) D. Craciunescu and colleagues pioneered a novel approach for diagnosing faults in PV arrays using Fuzzy C-Mean (FCM) clustering and fuzzy membership algorithms. This method facilitates the examination of electrical characteristics of PV systems under various fault scenarios [14]. 7) Hameed, et al. proposed an FLC model for implementing a PV peak power tracking system, thereby demonstrating its effectiveness [25]. Their research also involved constructing an analytical model for the PV system based on the manufacturer’s specifications. This approach incorporated a solar panel and converter model, along with a developed FLC algorithm designed for continuous maximum power tracking.

These valuable contributions collectively highlight the complex research landscape and varied strategies employed to improve the efficiency and performance of PV systems operating under shading conditions.

## 3. Methodological approach. Data and method

### 3.1. Numerical model of the PV solar cell

The application of the two-diode model’s mathematical framework reveals the intricate electrical properties of solar cells [52,53,54]. Various advanced models designed to account for specific conditions such as partial shading offer promising avenues for investigation [55,56]. One such model is the Bishop Model [57], which necessitates a negative voltage across its terminals, resulting in negative cell voltage and positive cell current—effectively consuming power. Conversely, the Direct Reverse Model [58] replicates solar cell behavior under various biasing modes to accommodate fluctuations in temperature and solar irradiance. This analysis addresses two main aspects: 1) the interaction between positive cell voltage and current, and 2) the contrast between negative cell voltage and positive cell current, which are critical for power analysis and estimating losses during partial shading scenarios. Future research could focus on optimization methods to tackle challenges in parameter estimation, potentially minimizing estimation errors and computational overhead.

In the operation of solar cells, various parameters play critical roles in determining their performance. Hence, a conventional solar cell model is used, which is illustrated in Fig. 2 and shows the current  $I_{cell}$  provided by the cell, denoted as:

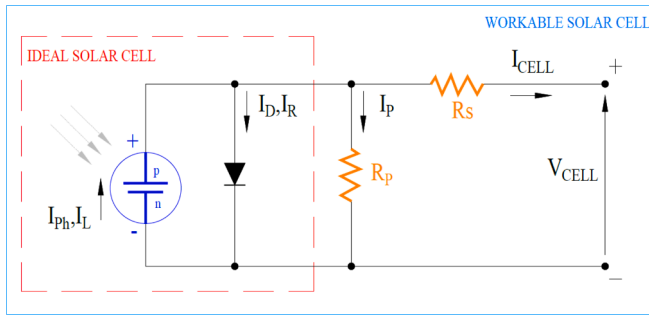


**Fig. 2.** The electrical schematic diagram of a solar cell, illustrating both the photo-sensitive and diode-type characteristics of the cell, along with the series and shunt resistances.

$$I_{cell} = I_{ph} - I_r - I_{sh} \quad (1)$$

where  $I_{ph}$ ,  $I_r$  and  $I_{sh}$  represent photo-generated current, reverse current, and shunt current – the current that bypasses the main circuit of the cell, often due to defects or non-ideal characteristics, negatively impacting overall efficiency. The voltage across the solar cell is denoted as  $V_{cell}$ , representing the electrical potential difference generated by the cell when it is exposed to light. In the context of the solar cell's operation, there is also a voltage  $V$  that develops across the shunt resistance  $R_{sh}$ . The relationship between these two voltages is expressed by the equation:  $V = V_{cell} + R_s I_{cell}$ , where  $R_s$  is the PV cell series resistance. The shunt current is given by  $I_{sh} = V/R_{sh}$ .

The classic diode theory provides the following values for the reverse current:

$$I_r = I_0 \left[ \exp \left( \frac{qV}{B_{cell} k T_{cell}} \right) - 1 \right] \quad (2)$$

where  $I_0$  represents the reverse saturation current,  $B_{cell}$  is the thermal voltage constant,  $K$  is the Boltzmann constant, and  $T_{cell}$  is the cell temperature. The electron's electric charge is also known as  $q$ . Given the connections Eq. (1) can be written as:

$$I_{module} = M I_{ph} - \frac{NR_{sh} + NR_s + MR_{smodule}}{NR_{sh} NR_{smodule}} V_{module} - M I_0 \left\{ \exp \left[ \frac{q \left[ \left( M + N \frac{R_s}{R_{sh} module} \right) + V_{module} + \left( NR_s + MR_{smodule} + N \frac{R_s R_{smodule}}{R_{sh} module} \right) I_{module} \right]}{NMB_{cell} k T_{cell}} \right]} - 1 \right\} \quad (9)$$

$$I_{cell} = I_{ph} - I_0 \left\{ \exp \left[ \frac{q(V_{cell} + R_s I_{cell})}{B_{cell} k T_{cell}} \right] - 1 \right\} - \frac{V_{cell} + R_s I_{cell}}{R_{sh}} \quad (3)$$

Silicon solar cells can be utilized with the following relationships:

$$I_{ph} = G_T \bullet (\tau \alpha) \bullet s A_{cell} \quad (4)$$

$$I_0 = K_{cell} A_{cell} T_{cell}^3 \exp \left( - \frac{E_g}{k T_{cell}} \right) \quad (5)$$

In Eq. (4)  $G_T$  ( $\tau \alpha$ ),  $s$  and  $A_{cell}$  respectively denote the global irradiance at the level of the solar cell, the effective transmittance-absorptance product, a constant, and the cell's surface area. Moreover,  $K_{cell}$  and  $E_g$  represent the band gap of the cell material and the cell constant, respectively [62].

### 3.2. Numerical model of the theoretical PV generator (panel)

In [49] several solar cell interconnection systems were evaluated from the perspective of stability and viability (i.e., the capacity to work continuously for a predefined period of time). These strategies included: (a) a simplified series-parallel PV array configuration comprising  $M$  parallel strings, each string consisting of  $N$  solar cells connected in series; (b) a cross-connected system derived from the series-parallel configuration by adding additional connections along each junction row; and (c) a bridge arrangement, where the solar cells are connected in a manner similar to a bridge rectifier configuration. The approach presented in this paper is specifically designed for the basic series-parallel configuration. However, it remains adaptable for implementation in other interconnection strategies. Fig. 3 illustrates a PV panel consisting of  $M$  parallel strings where each string contains  $N$  identical series solar cells. The relationship between the voltage across the PV panel denoted as  $V_{module}$  and the voltage across an individual solar cell denoted as  $V_{cell}$  is expressed by the following relation:

$$I_{cell} = \frac{V_{module} + I_{module} R_{smodule}}{N} \quad (6)$$

where  $R_{smodule}$  is the resistance in the module series. The module's shunt resistance is being current through at  $I'$ ,  $M$  – parallel strings and  $N$ - solar cells connected in series. The source of  $R_s$  shunt is:

$$I' = \frac{V_{module} + I_{module} R_{smodule}}{R_{smodule}} \quad (7)$$

and the current “ $I'$ “ is defined as:

$$I' = I_{cell} M = I_{module} + I' \quad (8)$$

By applying Eq. (3) for the solar cell and Eqs. (6)–(8) with algebraic manipulation, the resulting characteristics of the PV module  $I_{module}$ – $V_{module}$ , respectively module's current–voltage relationship can be derived (refer also to [56]).

An improved version of Eq. (4) where the module shunt resistance  $R_{sh}$  module was disregarded is Eq. (9), [49]. The PV module's  $P_{module}$  electric power output is provided by:

$$P_{module} = I_{module} V_{module} \quad (10)$$

The total PV module's energy balance is as follows:

$$M N A_{cell} S G T (\tau \alpha) - M N A_{cell} U_{cell} (T_{cell} - T_a) - I_{module} V_{module} = 0 \quad (11)$$

where  $T_a$  represents the ambient temperature, while  $U_{cell}$  and  $T_{cell}$  are average PV module values of the heat dissipation coefficient (convection) and the temperature of the solar cells. In Eq. (11), the first term denotes the rate of solar irradiance absorption by the PV module, while the second term is the heat flux transferred by convection from the solar cells to the ambient environment. Note that the second term includes all PV module resistances' Joule effect heat losses. The third term

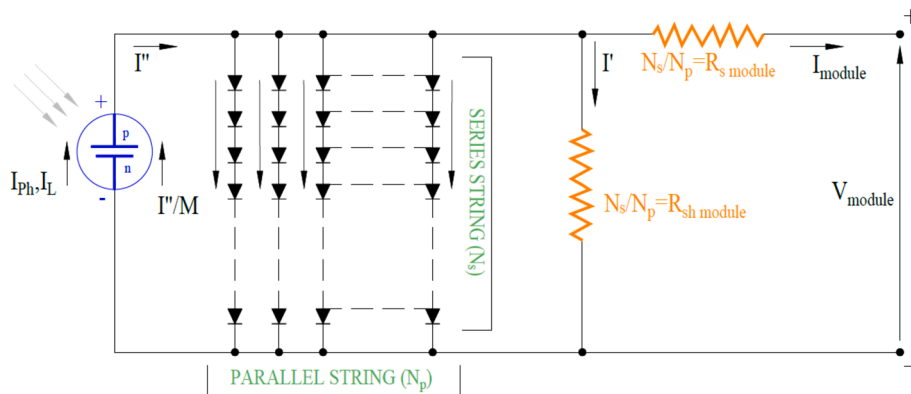


Fig. 3. The equivalent circuit diagram of a series-parallel PV module, featuring the series resistance ( $R_{S\_module}$ ) and shunt resistance ( $R_{Sh\_module}$ ).

represents electric energy leaving the PV module. The ratio of electrical output power and the incident solar radiation on the PV module represents the global efficiency  $\eta$  and is given by the Eq (12):

$$\eta = \frac{P_{module}}{G_T A_{module}} \quad (12)$$

where  $A_{module}$  = MNA<sub>cell</sub> determines the area of the PV module.

The quantitative and qualitative aspects related to the I-V curve, including  $I_{sc}$ ,  $V_{oc}$ , and MPP, are thoroughly investigated in the following sections. These analyses are conducted using numerical simulations with MATLAB/Simulink software.

### 3.3. Temperature influence on numerical model of the PV generator

The PV modules are generally used at temperatures ranging from  $-15\text{C} \div 60\text{C}$  and to even higher temperatures in space applications and concentrator systems. Many studies have pointed out that the performance of solar cells degrades as temperature increases. The variation of  $R_s$  and  $R_{sh}$  with temperature affects slightly efficiency.

In this paper, we analyze the variation of parameters  $V_{th}$  and  $I_0$  with temperature. The thermal voltage dependence on temperature is:

$$V_{th}^*(T) = \frac{k_B T}{q} = V_{th}^* \frac{T}{T^*} \quad (13)$$

where  $V_{th}^*$  is the thermal voltage at the standard temperature  $T = 298\text{ K}$ .

The reverse-bias saturation current depends on temperature according to Attivissimo [35]:

$$I_0(T)I_0^* = \left(\frac{T}{T^*}\right)^3 \exp\left[\frac{E_g}{q\gamma N_s V_{th}^*} \left(\frac{T - T^*}{T}\right)\right] \quad (14)$$

where  $E_g$  is the bandgap energy of the absorber layer  $I_0^* = I_0|_{T=T^*}$  and  $E_g$  depends on temperature by the relationship:

$$E_g(T) = E_g(0) - \frac{aT^2}{T + b} \quad (15)$$

where  $E_g(0)$  is the band gap value at  $T \approx 0\text{ K}$ , and  $a$  and  $b$  are constants. The values of the parameters in Eq. (15) are  $E_g(0) = 1.166\text{ eV}$ ,  $a = 4.73 \times 10 - 4\text{ eV/K}$  and  $b = 636\text{ K}$  [52]. The decrease of maximum output power is of 19.48 % for a temperature increase of 30 K, from  $T^* = 298\text{ K}$  to  $T = 328\text{ K}$ . This aspect is mainly due to the temperature dependence of the current  $I_0$  [Eq. (14)] that undergoes a rapid increase with temperature.

Temperature coefficient of the short circuit ( $I_{sc}$ ) characterizes how the short-circuit current varies with temperature changes. Elevated temperatures tend to enhance electron mobility, leading to a higher short-circuit current. Integrating this coefficient into models enhances their accuracy in forecasting current variations as the panel temperature

changes. This coefficient is particularly relevant in regions with significant temperature fluctuations. The research indicates that the temperature is a major factor in decreasing the PV panel performance [59], which has to be considered in panel design. Also, the studies from related literature clearly highlight temperature as a significant factor responsible for the decline in PV panel performance [60]. Consequently, one must account for temperature fluctuations to maximize the efficiency and longevity of PV systems. [61,62].

### 3.4. Investigation of the behavior and output events of PV generator

The methodology, detailed through a block diagram, guided the numerical modeling of the PV panel's electrical characteristics, including the I-V and P-V curves, as shown in Fig. 4's flowchart. This diagrammatic approach provided a clear and structured framework for the simulation process, ensuring that each step of the modeling was methodically planned and executed. A key benefit of this MATLAB-based approach is the ease with which the PV generator model can be integrated or adapted to evolving system models. In addition, MATLAB's extensive library of functions and toolboxes supports advanced and complex analysis of the PV panel's performance under various

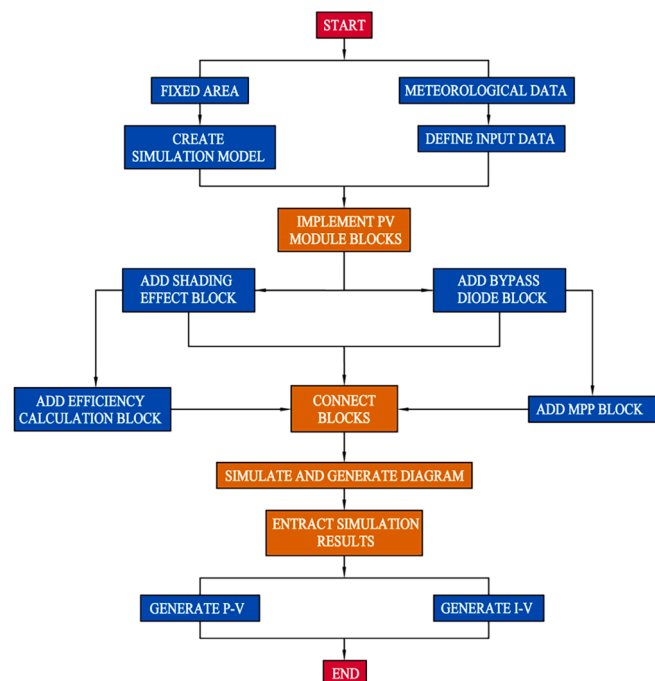


Fig. 4. Simulink flowchart.

**Table 1**

Comparison of the electrical characteristics and performances of the PV panel.

Parameters	U.M.	I-V Full Illuminated	I-V 80 % Illuminated	I-V 70 % Illuminated	I-V 60 % Illuminated
$V_{OC}$	(V)	43.36	43.36	43.36	43.36
$I_{SC}$	(A)	6.098	6.098	6.098	6.098
$P_{max}$	(W)	264.409	264.409	264.409	264.409
$P_{MPP}$	(W)	225.087	187.546	144.831	88.99
$V_{PM}$	(V)	37.76	37.66	37.56	39.36
$I_{PM}$	(A)	5.961	4.893	3.856	2.261
$FF$	(–)	0.851	0.709	0.547	0.336
$\eta$	(%)	22.508	17.410	14.48	8.89

conditions. This capability is essential for identifying potential inefficiencies and areas for improvement, thereby enhancing the overall performance of the PV system.

Power output optimization was examined under fixed area conditions. For consideration of the I-V and P-V curves characterizing the PV system under consideration, the authors developed a mathematical model that considers the influence of varying degrees of illumination (different shading conditions).

The simulation outcomes, which explored varying levels of shading (20 %, 30 %, 40 %), indicate that partial shading leads to a notable decrease in output power. These comprehensive results provide a detailed understanding of how shading influences the overall system performance and stability. **Table 1** presents the main parameters resulting from numerical simulations of the PV panel.

The results obtained using the MATLAB/Simulink programming environment are presented in **Fig. 5**, highlighting the PV system's sensitivity to reduced illumination variations (shading) and the non-uniform distribution of shading. Based on these results, it can be concluded that implementing optimization MPPT algorithms is crucial for maximizing output power.

#### 4. Numerical analysis of the industrial PV generator

##### 4.1. Modelling and simulation of an industrial PV generator

An industrial PV panel was analyzed based on the theoretical model discussed above. We analyzed a PV panel consisting of  $N_s = 144$  polycrystalline silicon cells.

The performance of a PV panel is analyzed by numerical simulation for AM 1.5 G solar spectrum and standard temperature conditions. The I-V curve with model parameters of **Table 2** is traced in **Fig. 6** and compared with that from the datasheet.

The analysis of the correlation coefficient, which exceeds 0.99, demonstrates a strong agreement between the modeled parameters and the empirical data derived from the PV panel's datasheet. This high correlation coefficient indicates that the model effectively captures the underlying physical behavior of the PV generator. The parameters utilized in this model, including Saturation Current ( $I_0$ ), Series Resistance ( $R_s$ ), Shunt Resistance ( $R_{sh}$ ), Ideality Factor ( $\beta_{PV}$ ) and Temperature Coefficient ( $\gamma$ ) are critical in evaluating the performance of PV generator under varying incident light flux power densities. These parameters are determined by fitting the Lambert W function to the datasheet data for the PV generator. The fitting program is based on the Levenberg-Marquardt method, which enhances the accuracy of the parameter estimation.

The application of the Levenberg-Marquardt method, a widely used nonlinear least squares fitting technique, enhances the robustness of the parameter estimation process. This methodological approach allows for precise fitting and adjustment of the model, ensuring that the

**Table 2**

Model parameters obtained by fitting Eq. (1) with the I-V curve from the datasheet.

Parameters	$I_0$ [A]	$R_s$ [ $\Omega$ ]	$R_{sh}$ [ $\Omega$ ]	$\gamma$	$\beta_{PV}$
	12.963	0.253	429.96	1.18	0.9

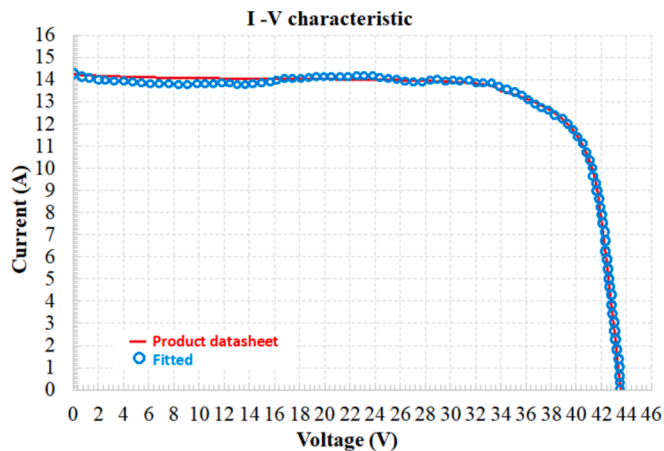


**Fig. 6.** I-V characteristic of the industrial PV panel for two cases: datasheet and fitted.

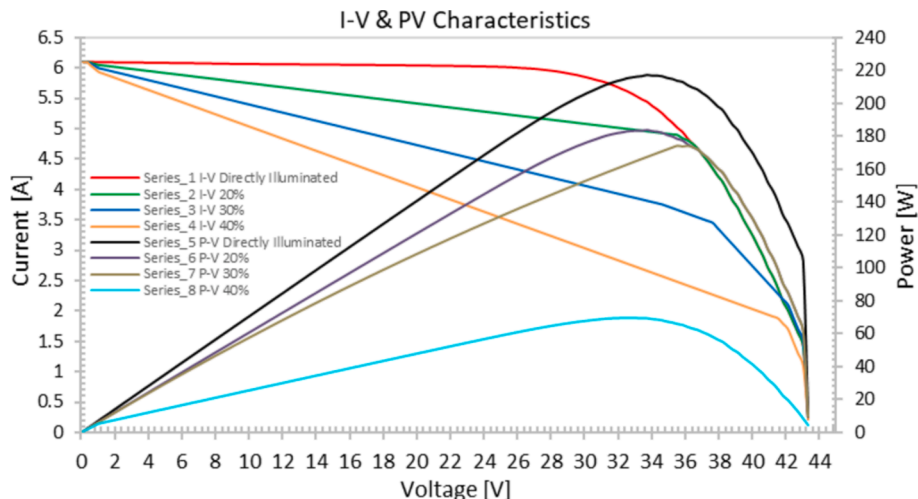


**Fig. 5.** The behavior of the I-V and P-V characteristics for different degrees of illumination (shading).

**Table 3**

Electrical characteristics &amp; performances of the PV generator.

Parameters		Datasheet value	Calculated value	Relative error [%]
$P_{max}$	[W]	560	532	5.348
–	[W]	0 ± 5	–	–
$V_{oc}$	[V]	50.2	49.3	1.793
$I_{sc}$	[A]	14.11	13.76	2.481
$V_{mp}$	[V]	42	43.528	-3.638
$I_{mp}$	[A]	13.35	13.81	-3.446
–	[A]	25	–	–
$T_N$	[°C]	43 ± 2	–	–
$N_{cells}$	[–]	144	–	–
FF	[%]	–	78.56	–
$\eta$	[%]	21.1	21.4	-1.422

parameters reflect the operational characteristics of the PV generator under real-world conditions.

The results are listed in [Table 2](#). A dedicated MATLAB software solves and computes the specific equation used for PV panel parameters: Short-Circuit Current ( $I_{sc}$ ), Open-Circuit Voltage ( $V_{oc}$ ), Fill Factor (FF), Maximum Power ( $P_{max}$ ) and Efficiency ( $\eta$ ).

It should be noted that the FF indicates the quality of the PV panel. The calculated FF value is 78.56 %, suggesting good panel quality. Additionally, the ( $\eta$ ) shows a slight improvement in the calculated value compared to the datasheet, indicating a potentially better performance than expected one (21.4 %). The relative error offers insights into potential discrepancies and areas for further refinement in the model. Such evaluations are essential for advancing the design and optimization of photovoltaic systems.

These values are presented in [Table 3](#) and compared with the datasheet ones (Industrial panel). By comparing the calculated values with those provided in the datasheet of the industrial panel, it becomes possible to evaluate the accuracy of the fitting model.

In conclusion, the strong correlation coefficient and the resulting parameter estimates underline the effectiveness of the model in assessing PV panel performance.

#### 4.2. Experimental approach of the electrical characteristics of PV generator

This chapter sets the stage for a holistic exploration into the assessment of PV potential across in Constanta city, Romania – a country in Eastern Europe, on the Black Sea shore, with great PV potential.

Recognizing the complex interplay of the environmental variables, the primary objective is to present an integrated framework that balances computational efficiency with precision.

The measurements serve as a benchmark to validate the accuracy of the simulation models. By comparing modelled results against actual measurements, we can refine and calibrate the models, as well as improving the predictive capabilities. High-quality data contributes significantly to achieving a reliable level of approximation and enhances precision, especially when contrasted with directly observed values. By combining the use of average data, site-specific validation, and trend analysis, this research aims to provide a large view regarding the performance and operation optimization of PV generators and could be considered suitable and applied in many investigations.

The accuracy of the results is contingent on both the quality of data sources and the refinement of the trained models utilized in simulations.

In order to investigate the dynamic behavior of the proposed PV generator, the authors used MATLAB/Simulink, environment incorporating MPPT techniques and a specific MPPT algorithm. The authors have conducted a study to investigate the influence of varying incident solar irradiance flux power densities on the current–voltage characteristic of a PV system.

The study also considered the impact of temperature as described in the mathematical model presented in Section 3.3. [Table 4](#) presents a set of 100 measured values for irradiance and another 100 measured values for temperature. Subsequently, the collected data facilitated a comprehensive comparison and optimization of the PV generator, which is illustrated in [Fig. 5](#).

[Fig. 7](#) provides a detailed analysis of the voltage and output power behavior, demonstrating the impact of an operational optimization method based on the MPPT (Maximum Power Point Tracking) technique. The figure can be interpreted as follows:

**Voltage Behavior (top plot):** The top plot illustrates how panel voltage changes under different conditions and highlights the optimization gain achieved through the MPPT process. The datasheet voltage (orange line) remains nearly constant, just below 45 V, which represents the ideal voltage specified by the manufacturer under Standard Test Conditions (STC). This voltage is stable because it assumes ideal, constant conditions that aren't replicated in the real-world experimental setup. The fitted voltage (cyan circles) remains relatively stable around 45 V throughout the time period, representing a best-fit voltage model that serves as an ideal reference. In contrast, the measured/experimental voltage (blue line) fluctuates more, which is expected under real conditions influenced by environmental factors. The MPPT-optimized

**Table 4**

Meteorological raw data (solar irradiance and temperature) for clear sky and partial cloudy sky.

Irradiance Data (W/m <sup>2</sup> )										Temperature Data (°C)									
Sunny Day Solar					Partly Sunny Day					Sunny Day Ambient					Partly Sunny Day				
1100	1005	1050	1000	1060	650	605	655	600	660	33.5	36.3	33.8	37.2	47.1	22.8	23.1	22.4	22.8	23.1
1050	1020	1035	1085	1045	600	620	640	685	645	40.2	48.2	50.0	49.7	36.1	21.5	22.1	21.0	21.5	22.1
1150	1045	1125	1090	1015	700	645	715	690	615	42.8	49.8	39.5	34.4	49.4	23.7	21.9	23.5	23.7	21.9
1125	1110	1110	1035	1000	725	710	710	645	600	38.7	37.1	34.3	44.0	44.4	22.0	23.2	24.1	22.0	23.2
1080	1095	1080	1065	1150	680	700	685	665	725	36.4	38.5	47.0	40.0	33.0	24.5	22.5	22.7	24.5	22.5
1130	1135	1100	1040	1105	730	740	705	640	685	48.9	40.9	40.7	45.0	42.5	21.8	21.4	21.3	21.8	21.4
1115	1055	1120	1155	1125	715	630	725	755	705	45.6	34.0	42.1	42.6	46.2	23.3	23.4	23.9	23.3	23.4
1090	1040	1025	1120	1075	690	625	625	725	675	37.9	47.9	36.8	39.9	45.7	22.2	22.3	22.6	22.2	22.3
1075	1165	1010	1030	1135	675	755	610	635	740	44.2	49.1	39.3	46.0	40.3	22.9	21.6	21.7	22.9	21.6
1125	1145	1170	1025	1050	725	735	770	630	655	39.1	37.3	35.6	35.2	38.1	23.6	23.8	24.3	23.6	23.8
1060	1140	1140	1145	1080	640	730	735	750	685	36.7	33.9	41.3	48.5	35.0	22.4	22.8	23.1	22.4	22.8
1035	1000	1030	1175	1035	615	600	635	770	640	47.3	42.7	44.6	41.1	33.7	21.0	21.5	22.1	21.0	21.5
1190	1015	1190	1020	1020	790	615	790	620	625	42.0	36.5	49.5	45.5	37.6	23.5	23.7	21.9	23.5	23.7
1010	1025	1185	1095	1195	610	625	780	695	790	41.5	45.3	46.3	47.6	34.2	24.1	22.0	23.2	24.1	22.0
1175	1195	1060	1115	1180	770	790	660	715	775	35.8	41.8	37.7	34.6	39.6	22.7	24.5	22.5	22.7	24.5
1060	1185	1075	1100	1040	760	780	675	700	645	43.7	44.9	38.4	43.8	41.9	21.3	21.8	21.4	21.3	21.8
1030	1165	1130	1055	1010	635	755	725	655	610	46.5	46.7	32.0	39.7	48.4	23.9	23.3	23.4	23.9	23.3
1180	1095	1160	1070	1170	780	700	760	670	770	34.9	38.0	48.6	37.8	40.4	22.6	22.2	22.3	22.6	22.2
1085	1070	1150	1165	1160	665	675	750	760	760	39.8	43.2	43.4	38.8	43.0	21.7	22.9	21.6	21.7	22.9
1105	1075	1005	1180	1065	695	680	605	775	665	32.6	48.1	33.5	32.9	48.3	24.3	23.6	23.8	24.3	23.6

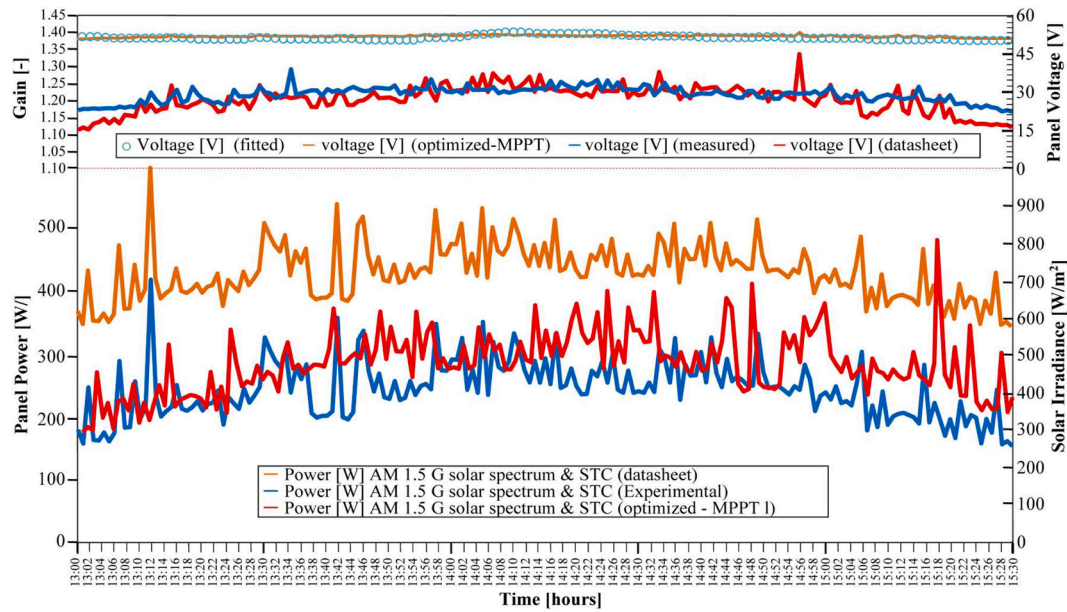


**Fig. 7.** Temporal analysis of PV generator performance: comparative evaluation of gain, voltage, and power based on experimental data, datasheet values, and MPPT optimization.

voltage (orange-red line) fluctuates between 35 V and 40 V, reflecting the real-time adjustments made by the MPPT system to maintain efficient panel operation under varying conditions. It's also noteworthy that the measured voltage closely tracks the MPPT-optimized voltage, demonstrating the effectiveness of the optimization. On the left axis, the gain shows how much improvement is achieved through the MPPT process. It remains stable above 1.2, peaking at around 1.35, indicating that the MPPT technique improves voltage efficiency by approximately 20–35 %.

**Power Output Behavior (bottom plot):** The bottom plot represents the output power as a function of solar irradiance. The datasheet power (orange line) reflects the ideal power output under STC, fluctuating but generally stable between 400 W and 500 W. This curve represents the expected power production under ideal, consistent conditions. The experimental power (blue line) shows the actual power generated by the panel under real conditions. This line is more volatile, frequently dropping below 300 W, and follows a similar pattern to the fluctuating

solar irradiance throughout the time period, highlighting the difficulty of maintaining consistent power output in varying sunlight conditions.

The MPPT-optimized power (red line) fluctuates within the 300 W to 400 W range. Although it is variable, the optimized power generally stays higher than the experimental one, demonstrating the benefits of the MPPT technique in boosting overall power output.

In both plots, the orange and red curves (representing datasheet and MPPT-optimized values) clearly demonstrate how the MPPT system optimizes performance. By dynamically adjusting the voltage, it helps maintain higher and more stable power production compared to the unoptimized experimental conditions. Overall, Fig. 7 underscores the advantages of MPPT optimization in stabilizing voltage and increasing power output, despite the challenges posed by fluctuating solar irradiance. While the optimized power consistently outperforms the experimental one, it does not reach the datasheet's ideal power, as expected, due to real-world factors such as changing irradiance, temperature variations, occasional shading, and material quality.

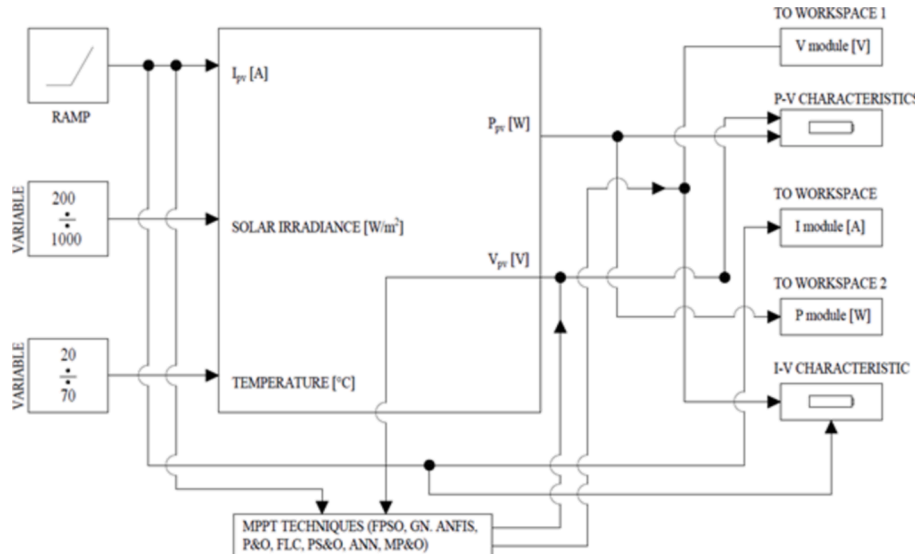


**Fig. 8.** Conceptual block diagram of implemented in MATLAB/Simulink.

## 5. Advanced numerical modelling method of the electrical characteristics of the PV generator based on MPPT techniques

### 5.1. Optimization procedure

The application of Maximum Power Point Tracking (MPPT) techniques involves eight algorithms, namely: Perturb and Observe (P&O), Modified Perturb and Observe (MP&O), Particle Swarm Optimization (PSO), Genetic Algorithm (GN), Fuzzy Logic Controller (FLC), Artificial Neural Network (ANN), Fuzzy Particle Swarm Optimization (FPSO), and Adaptive Neuro-Fuzzy Inference System (ANFIS), categorized into four distinct groups. These algorithms continually assess the actual output power of the PV generator against a reference power and an estimated peak power at specified intervals. The controller then adjusts the power reference, accordingly, adding it to the previous value at each interval.

The highest identified power value is deemed the maximum. The controller's output is converted into a Pulse Width Modulation (PWM) signal to regulate the voltage duty cycle, optimizing the PV system's performance at its peak power. The MPPT techniques based on the algorithms proposed in the paper were implemented in MATLAB using specific software tools, such as the Simulink module. Parameters for inputs and outputs, along with the MPPT algorithms' calculation models, were set up in the software's GUI editor.

A conceptual PV generator model was created in MATLAB /Simulink v\_R2021 to outline its electrical properties (see Fig. 8).

The inputs for the optimization procedure are as follows: One knows the climate where the PV application is implemented and the utilization period (here a yearly operation is assumed). Therefore, information about the average available solar irradiation during the period is known. The average electrical power to be provided during the period by the PV module is a choice.

The MPPT algorithm compares the actual power of the PV system ( $P_{PV}$ ) with the reference power (maximum one) ( $P_r$ ) – estimated value, via the MPPT controllers, at equal time intervals. The output of the MPPT controllers can direct the reference power to a new value, which is added to the previous value of each interval. The highest value can be considered as the maximum one. The output from the MPPT controllers is routed to a PWM signal (Pulse Width Modulation) to control the operating cycle of the DC-DC voltage converter. This device raises the voltage to a value at which the PV system can operate at full power. The FLC-based MPPT technique was implemented based on tool/library from MATLAB/Simulink. The first step is to define the MPPTs parameters (inputs, outputs) and methods (e.g.: rules, fuzzification and defuzzification in the case of FLC).

After the creation of the MPPT controllers in the MATLAB/Simulink, based on considered algorithms we made the controller configuration for each component of the PV system. In Fig. 9 for example the diagram of the MPPT controller is shown, where we have:  $P_{PV}$  – actual power of the PV system,  $I_{PV}$  – the current in the system,  $V_{PV}$  – the system voltage,  $P_r$  – the maximum estimated reference power, and  $S$  – the MPPT signal. In Fig. 10 the logic diagram is presented for implementing the control algorithm MATLAB / Simulink; the input to the MPPT controller is determined by the estimated reference power ( $P_r$ ) and PV system actual power ( $P_{PV}$ ), while the output from the MPPT is determined by the command signal ( $S$ ).

### 5.2. Response of the PV generator to eight MPPT algorithms

In accordance with the data provided by Fig. 1 of Chapter 1, a selection of algorithms representing each category (Classical Method, Optimization Method, Advanced Method, and Hybrid Method) was made for the purpose of comparative analysis. The aim was to assess their respective performances and determine the most suitable algorithm for investigating the shadow effect, as discussed in the subsequent chapter of this article. Given that the first category held limited interest, the most representative algorithms, denoted as P&O and MP&O, were

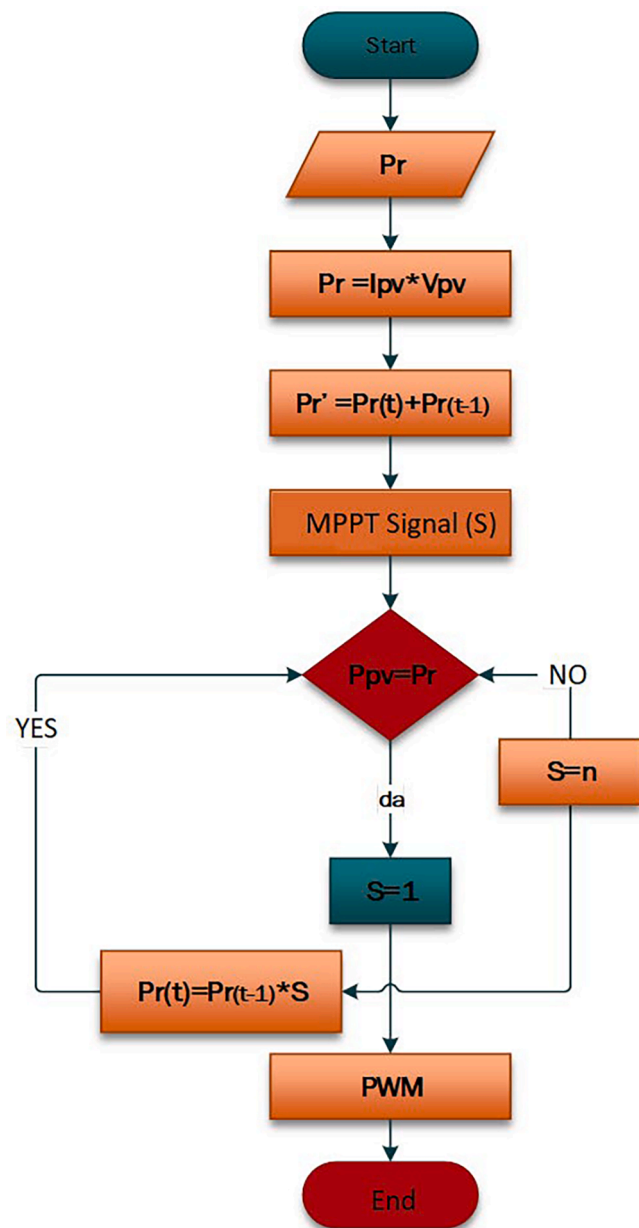


Fig. 9. MPPT controller configuration.

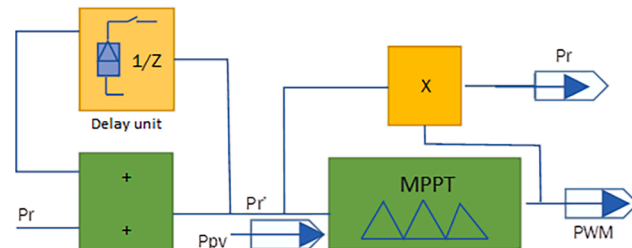


Fig. 10. Logic diagram for implementing the control algorithms in MATLAB/Simulink.

chosen as a reference. From the remaining three categories, two algorithms were selected, specifically from Category 2 – PSO and GN, Category 3 – FLC and ANN, and Category 4 – FPSO and ANFIS. In total, eight distinct MPPT algorithms were subjected to comparison and

**Table 5**  
Weather conditions.

Approach	Irradiation (G)	Temperature (T)
Dynamic weather	100 to 1000 W/m <sup>2</sup> (Fig. 11)	25 °C
	100 to 1000 Wm <sup>2</sup> (Fig. 11)	10 to 65 °C (Fig. 12)

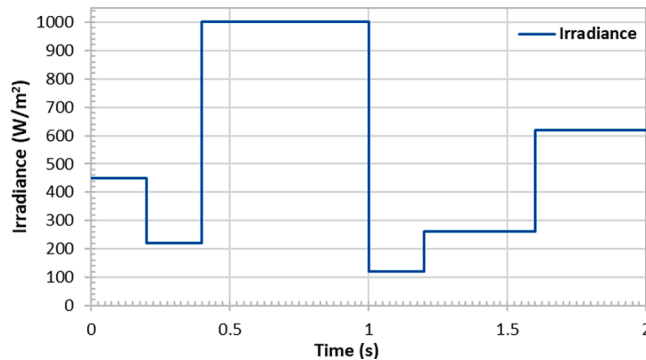


Fig. 11. Weather condition: solar irradiance.

analysis. Consequently, P&O, MP&O, PSO, GN, FLC, ANN, FPSO, and ANFIS controllers were created and simulated using MATLAB/Simulink. The simulation results reveal an increase in both the power output of the PV device and the overall power generated by the PV panel. These outcomes, when viewed in the context of PV panel power output, assume a critical role in the determination of electrical characteristics and the corresponding system efficiency concerning electricity generation. The authors of this study conducted a performance comparison of the PV panel, employing four distinct categories of MPPT algorithms, as mentioned above. This comparative analysis underscores the significant role that MPPT algorithms play in optimizing the performance of PV systems.

To investigate the power behavior of the generator, Table 5 provides an overview of weather conditions. Utilizing experimental data obtained

from the inverter and detailed in Chapter 4, they were able to accurately determine the solar irradiance, as illustrated in Fig. 11.

Additionally, experimental temperature data were incorporated into this analysis, as shown in Fig. 12. These graphical representations of solar irradiance and temperature were instrumental in conducting a comprehensive comparison and evaluation of the eight MPPT algorithms selected from the four categories discussed in this article, as described in Fig. 1.

In Fig. 13 is presented the performance metrics recorded by the controllers in terms of power gain for the entire PV generator. Although the P&O and MP&O indicates weak performances, while PSO and GN, indicate medium performances, FLC and ANN, indicate good performances, while the FPSO and ANFIS techniques deliver excellent performance under fluctuating irradiance conditions.

The simulation times for each MPPT method were recorded using MATLAB's built-in tic-toc command, providing a measure of the time required for MATLAB to execute the relevant code.

Furthermore, Fig. 13 reveals that the maximum power output recorded by the PV generator diverges from the manufacturer's specified rating of 560 Wp (ideal standardized test conditions).

This variance can be attributed to the impact of actual environmental conditions, including fluctuations in solar irradiance and temperature.

The simulation results indicate a maximum power output of 501.23 W under dynamic real-time conditions. This numerical modeling holds particular significance as it provides an accurate estimate of the PV generator's performance within genuine operational scenarios, emphasizing stability and power peak enhancement.

This numerical modeling holds particular significance as it provides an accurate estimate of the PV generator's performance within genuine operational scenarios, emphasizing the realized power enhancement.

There are two major transitions in solar irradiance: one at approximately 0.5 s (increase) and another at 1.2 s (decrease). During these transitions, all algorithms demonstrate a transient response, with minor overshoots before stabilizing. In particular, around 1.2 s, when the solar irradiance drops, all algorithms show a corresponding drop in power output. However, the ANFIS and FPSO algorithms seem to recover the fastest and most efficiently, reaching a stable steady state sooner than others.

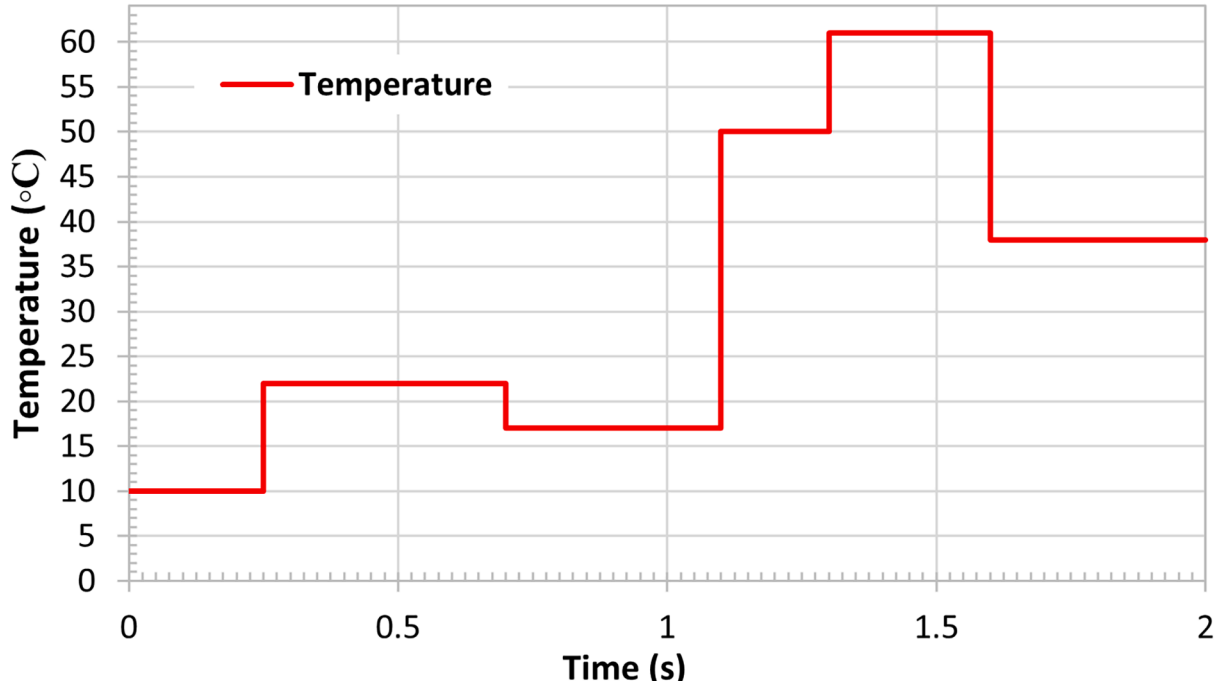
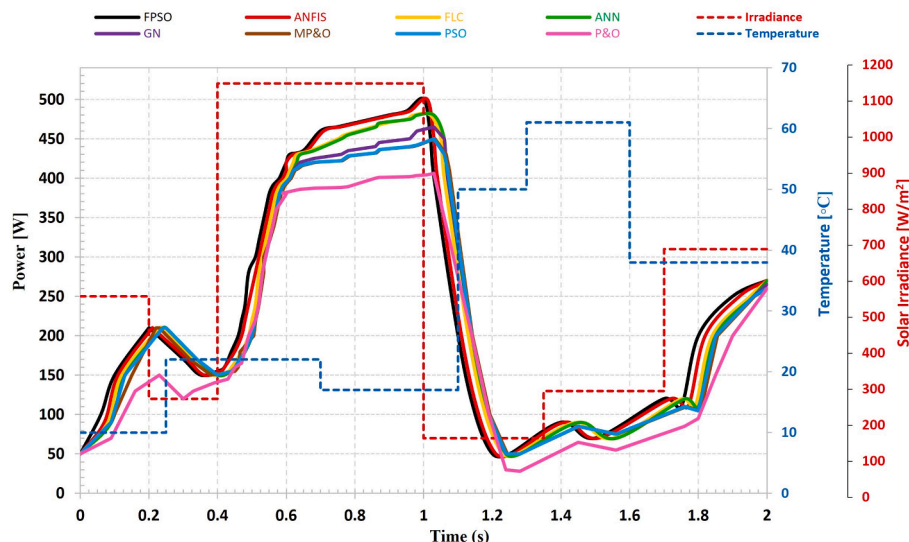


Fig. 12. Weather condition: temperature.



**Fig. 13.** Comparative analysis of the power-time representation of the maximum power point (MPP) for a PV generator under dynamic irradiance and temperature conditions, evaluating the adaptability of eight distinct MPPT algorithms (FPSO, GN, ANFIS, P&O, FLC, PSO, ANN, MP&O) to sudden variations in operating conditions.

The FPSO and ANFIS techniques deliver the best results and demonstrate improved accuracy with values closely matching those of the PV generator (very close to the industrial PV panel datasheet values). Solar irradiance values from Table 4 (Sunny Day Solar and Partially Sunny Day) collected over a 2.5-hour period were considered to establish the highest power point and lowest MPP point (412 and 927 W/m<sup>2</sup>).

To evaluate the robustness of these controllers, simulations also considered variable temperatures ranging between 21.3 °C and 50.0 °C.

## 6. Discussions and Conclusions

The authors conducted a comprehensive analysis, exploring various aspects such as the influence and behavior of different shading levels on the performance of the PV generator. Additionally, a comparative analysis was performed between the experimental data, the datasheet values, and the results obtained through operational optimization based on the MPPT technique. The study demonstrated and validated the usefulness of optimizing generators, in terms of gains and power output efficiency.

The study focused on enhancing existing techniques to optimize the performance of the PV generator through MPPT algorithms, aimed at maximizing electrical energy extraction from a PV system. In contrast to other studies in the literature [31], which predominantly depend on a three-point optimization approach for extracting the MPP, our approach leverages five operational points. The previous research analyzed the limitations of the rudimentary three-point operation, highlighting its instability at the MPP under dynamic conditions. By assessing five points on the P-V curve, as explored in prior research, our algorithm fine-tunes its operation, reducing significant oscillations around the MPP, improving stability, and minimizing energy loss [14]. Additionally, adopting the five-point operation enables the system to detect subtle changes in meteorological conditions (solar irradiance, temperature), allowing for smoother adjustments.

The new advancement presented in this study consists in a comparative analysis of eight different algorithms. The results revealed that the ANFIS technique exhibits superior response times, while MP&O, GN, PSO, ANN, and FLC demonstrate good adaptability to both sudden increases and decreases in irradiance, with acceptable oscillation and delay in reaching optimal performance, except for P&O. Both ANFIS and FPSO demonstrated performance in relation to the leading methods found in the literature.

This comprehensive approach not only improves electrical output parameters but also provides valuable insights into managing sudden fluctuations in solar irradiance. This novel insight explores the impact of different MPPT techniques on the PV generator's output power, achieving operational optimization that closely aligns with the real operating conditions of the PV system.

The implications of our findings are substantial, offering direct benefits for enhancing output power. The results efficiently integrate both qualitative and quantitative aspects, suggesting broad applicability across various contexts, including both autonomous and grid-connected PV systems. Overall, this distinct perspective represents a significant contribution to the field, providing a validated framework for optimizing PV generator performance through algorithmic enhancements.

## Appendix A. Supplementary data

Supplementary data to this article can be found online at <https://www.mdpi.com/1996-1073/16/3/1169>.

## Declaration of generative AI and AI-assisted technologies in the writing process

During the preparation of this work the authors used ChatGPT in order to translate some sentences from Romanian to English. After using this tool/service, the authors reviewed and edited the content as needed and took full responsibility for the content of the publication.

## CRediT authorship contribution statement

**Ana-Maria Badea:** Writing – original draft, Software, Resources, Methodology, Investigation, Data curation. **Doina Manaila-Maximean:** Writing – review & editing, Visualization, Validation, Supervision, Project administration, Methodology, Investigation, Formal analysis, Data curation, Conceptualization. **Laurentiu Fara:** Writing – review & editing, Visualization, Validation, Supervision, Project administration, Methodology, Formal analysis, Conceptualization. **Dan Craciunescu:** Writing – original draft, Software, Resources, Investigation.

## Declaration of Competing Interest

The authors declare the following financial interests/personal

relationships which may be considered as potential competing interests: [Ana-Maria Badea reports article publishing charges and travel were provided by National University of Science and Technology Politehnica Bucharest. If there are other authors, they declare that they have no known competing financial interests or personal relationships that could have appeared to influence the work reported in this paper].

## Acknowledgements

Ana-Maria Badea would like to acknowledge the financial support granted by the National University of Science and Technology Politehnica Bucharest, Romania in the form of a Ph. D. scholarship (Doctoral Contract No: SD12/4/02/10/2024).

## References

- [1] M. Etarhouni, et al., Design of novel differential power processing scheme for small-scale PV array application operating under partial shading conditions: modelling and experimental validation, *Comput. Electrical Eng.* 117 (2024). ISSN 0045-7906.
- [2] L. Fara, et al., Forecasting of energy production for photovoltaic systems based on ARIMA and ANN advanced models, *Int. J. Photoenergy* (2021) 1–19.
- [3] L. Fara, et al., Forecasting of energy production and operational optimization for photovoltaic systems, *Ann. Acad. Romanian Scientists* 3 (1) (2018) 31–60. ISSN 2559-1061.
- [4] L. Fara, D. Craciunescu, S. Fara, Numerical modelling and digitalization analysis for a photovoltaic pumping system placed in the south of Romania, *Energies* 14 (10) (2021) 2778.
- [5] L. Fara, D. Craciunescu, Output analysis of stand-alone PV systems: modeling simulation and control sustainable solutions for energy and environment, *Energy Procedia* 112 (2017) 595–605.
- [6] L. Fara, et al., Results in performance improvement and operational optimization of photovoltaic components and systems, *Ann. Acad. Rom. Sci. Ser. Phys. Chem. Sci* 2 (2017) 7–30. ISSN 2559-1061.
- [7] D. Craciunescu, et al., Optimized Management for Photovoltaic Applications Based on LEDs by Fuzzy Logic Control and Maximum Power Point Tracking Springer International Publishing AG 2018 Nearly Zero Energy Communities Springer Proceedings in Energy, pp 317–336 (2018).
- [8] X. Fang, et al., Dynamic reconfiguration of photovoltaic array for minimizing mismatch loss, *Renew. Sustain. Energy Rev.* 191 (2024). ISSN 1364-0321.
- [9] A. Mansouri, A. El Magri, R. Lajouad, F. Giri, A. Watil, Nonlinear control strategies with maximum power point tracking for hybrid renewable energy conversion systems, *Asian J. Control* 26 (2) (2024) 1047–1056.
- [10] O. Tofopefun, et al., Photovoltaic modeling: a comprehensive analysis of the I-V characteristic curve, *Sustainability* 16 (1) (2024) 432.
- [11] A. Bárar, et al., Parameter extraction of an organic solar cell using asymptotic estimation and Lambert W function. In: *Advanced Topics in Optoelectronics, Microelectronics, and Nanotechnologies VIII* (Vol. 10010, pp. 799–805). SPIE (2016).
- [12] S. Leihou, et al., A horizontal single-axis tracking bracket with an adjustable tilt angle and its adaptive real-time tracking system for bifacial PV modules, *Renewable Energy* 221 (2024). ISSN 0960-1481.
- [13] H. Oufetouli, et al., Comparative Performance Analysis of PV Module Positions in a Solar PV Array Under Partial Shading Conditions, “, *IEEE Access* 11 (2023) 12176–12194.
- [14] D. Craciunescu, L. Fara, Investigation of the Partial shading effect of photovoltaic panels and optimization of their performance based on high-efficiency FLC algorithm, *Energies* 16 (3) (2023) 1169.
- [15] E. Gouvéa, et al., Performance analysis of interconnection and differential power processing techniques under partial shading conditions, *Energies* 17 (13) (2024) 3252.
- [16] J. Vandana, Generalized modelling of PV module and different PV array configurations under partial shading condition, *Sustain. Energy Technol. Assessments* 56 (2023). ISSN 2213-1388.
- [17] B. Naveen, T. Manoj, A novel adaptive and modified controller for tracking global peak under partial shading conditions, *Comput. Electrical Eng.* 118 (Part A) (2024) 109372. ISSN 0045-7906.
- [18] G. Gennaro, et al., Modelling double skin façades (DSFs) in whole-building energy simulation tools: validation and inter-software comparison of naturally ventilated single-story DSFs, *Build. Environ.* 231 (2024). ISSN 0360-1323.
- [19] F. Nicoletti, M.A. Cucumo, N. Arcuri, Building-integrated photovoltaics (BIPV): a mathematical approach to evaluate the electrical production of solar PV blinds, *Energy* 263 (2023). ISSN 0360-5442.
- [20] F. Belhachat, C. Larbes, Photovoltaic array reconfiguration strategies for mitigating partial shading effects: recent advances and perspectives, *Energy Conv. Manag.* 313 (2024) 118547. ISSN 0196-8904.
- [21] A. Ziane, et al., Photovoltaic output power performance assessment and forecasting: impact of meteorological variables, *Solar Energy* 220 (2021) 745–757. ISSN 0038-092X.
- [22] T. Skaif, A systematic analysis of meteorological variables for PV output power estimation, *Renew. Energy*, Elsevier (2020).
- [23] H. Rezk, et al., A comparison of different global MPPT techniques based on meta-heuristic algorithms for photovoltaic system subjected to partial shading conditions, *Renew. Sustain. Energy Rev.* 74 (2017) 377–386.
- [24] Z. Abderrezzag, et al., Photovoltaic output power performance assessment and forecasting: impact of meteorological variables, *Solar Energy* 220 (2021) 745–757. ISSN 0038-092X.
- [25] R. Hameed, et al., A structured review of MPPT Techniques for Photovoltaic systems, *AIP Conference Proceedings*, AIP Publishing, 2023.
- [26] N. Karami, N. Moubayed, R. Outbib, General review and classification of different MPPT Techniques, *Renew. Sustain. Energy Rev.* 68 (2017) 1–18. ISSN 1364-0321.
- [27] D. Sharma, M.F. Jalil, M.S. Ansari, R.C. Bansal, A review of PV array reconfiguration techniques for maximum power extraction under partial shading conditions, *Optik* 275 (2023). ISSN 0030-4026.
- [28] H. Oufetouli, et al., Comparative performance analysis of PV module positions in a solar PV array under partial shading conditions, *IEEE Access* 11 (2023) 12176–12194.
- [29] D.P. Winston, S. Kumaravel, B.P. Kumar, S. Devakirubakaran, Performance improvement of solar PV array topologies during various partial shading conditions, *Solar Energy* 196 (2020) 228–242. ISSN 0038-092X.
- [30] H. Hanifi, et al., A novel electrical approach to protect PV modules under various partial shading situations, *Sol. Energy* 193 (2019) 814–819.
- [31] R. K. Pachauri, et al., Investigation on SP and TCT Photovoltaic Array Configurations under Obscured Shading Conditions, 2020 IEEE 7th Uttar Pradesh Section International Conference on Electrical, Electronics and Computer Engineering (UPCON), Prayagraj, India, pp. 1–6, (2020).
- [32] G. Vieira, et al., A comprehensive review on bypass diode application on photovoltaic modules, *Energies* 13 (10) (2020) 2472.
- [33] A. Bárar, et al., Stochastic modelling of hopping charge carrier transport mechanism in organic photovoltaic structures. In: *Photonics for Solar Energy Systems VII* (Vol. 10688, pp. 8–14), SPIE (2018).
- [34] C. Saiprakash, A. Mohapatra, B. Nayak, S.R. Ghatak, Analysis of partial shading effect on energy output of different solar PV array configurations, *Mater. Today: Proc.* 39 (2021) 1905–1909. ISSN 2214-7853.
- [35] V. Badescu, Simple optimization procedure for silicon-based solar cell interconnection in a series-parallel PV module, *Energ. Conver. Manage.* 47 (2006) 1146–1158.
- [36] L. Fara, D. Craciunescu, A. Diaconu, Results in performance improvement and operational optimization of photovoltaic components and systems, *Ann. Acad. Rom. Sci. Ser. Phys. Chem. Sci* 2 (2017) 7–30. ISSN 2559-1061.
- [37] M. Premkumar, U. Subramaniam, T.S. Babu, R.M. Elavarasan, L. Mihet-Popa, Evaluation of mathematical model to characterize the performance of conventional and hybrid PV array topologies under static and dynamic shading patterns, *Energies* 13 (12) (2020) 3216.
- [38] J. Bishop, Computer simulation of the effects of electrical mismatches in photovoltaic cell interconnection circuits, *Sol. Cells* 25 (1988) 73–89.
- [39] V. Jha, Comprehensive modeling and simulation of PV module and different PV array configurations under partial shading condition, *Iran J. Sci. Tech. Trans. Electrical Eng.* 46 (2022) 503–535.
- [40] W. Kreft, et al., Reduction of electrical power loss in a photovoltaic chain in conditions of partial shading, *Opt. Int. J. Light Electron. Opt.* 202 (2019) 163559.
- [41] V. Badescu, Time dependent model of a complex PV water pumping system, *Renew. Energy* 28 (2003) 543–560.
- [42] V. Badescu, Maximum work rate extractable from energy fluxes, *J. Non-Equilib. Thermodyn.* (2021).
- [43] V. Badescu, Spectrally and angularly selective photothermal and photovoltaic converters under one-sun illumination, *J. Phys. D Appl. Phys.* 38 (2005) 2166–2172.
- [44] A. Barar, D. Manaila-Maximean, M. Vladescu, P. Schiopu, Simulation of charge carrier transport mechanisms for quantum dot-sensitized solar cell structures, *Univ. Politeh. Buchar. Ser. A* 81 (2019) 265–270. ISSN 1223-7027.
- [45] A. Bárar, Thermal behavior of the electrical parameters for a novel zinc derivative-based dye-sensitized solar cell. In: *Advanced Topics in Optoelectronics, Microelectronics, and Nanotechnologies IX* (Vol. 10977, pp. 177–181), SPIE, (2018).
- [46] R. Ahmad, et al., An analytical approach to study partial shading effects on PV array supported by literature, *J. Renew. Sustain. Energy Rev.* 74 (2017) (2017) 721–732.
- [47] T. Sebbagh, et al., An experimental validation of the effect of partial shade on the I-V characteristic of PV panel, *Int. J. Adv. Manuf. Technol.* 96 (2018) 4165–4172.
- [48] T. Betti, A. Kristić, I. Marasović, V. Pekić, Accuracy of simscape solar cell block for modeling a partially shaded photovoltaic module, *Energies* 17 (10) (2024) 2276.
- [49] M.Z. Ramli, Z. Salam, Performance evaluation of dc Power optimizer (SCPO) for photovoltaic (PV) system during partial shading, *Renew. Energy* 139 (2019) 1336–1354.
- [50] A. Barar, et al., Two-diode modelling of perovskite solar cells and parameter extraction using the lambert w function, *University Politehnica of Bucharest Scientific Bulletin-Series A-Applied Mathematics and Physics*, 83(4), pp.285-294, ISSN 1223-7027, (2021).
- [51] A. Omar, et al., Solar photovoltaic energy optimization methods, challenges and issues: a comprehensive review, *J. Clean. Production* 284 (2021). ISSN 0959-6526.
- [52] T. Sebbagh, R. Kelaiaya, A. Zaatri, An experimental validation of the effect of partial shade on the I-V characteristic of PV panel, *Int. J. Adv. Manuf. Technol.* 96 (2018) 4165–4172.
- [53] A. Barar, D. Manaila-Maximean, Ruthenium-based DSSC efficiency optimization by grapheme quantum dot doping, *Univ. Politeh. Buchar. Sci. Bull. Ser. A Appl. Math. Phys* 2 (2021) 309–316. ISSN 1223-7027.

- [54] P. T. Landsberg, V. Badescu, Some methods of analyzing solar cell efficiencies Thermodynamics of Energy Conversion and Transport ed S Sieniutycz and A De Vos (New York: Springer) pp 46-49, (2000).
- [55] V. Badescu, P.T. Landsberg, C. Dinu, Thermodynamic optimisation of non-concentrating hybrid solar converters, *J. Phys. D Appl. Phys.* 29 (1996) 246–252.
- [56] O. Bingöl, B. Ozkaya, Analysis and comparison of different PV array configurations under partial shading conditions, *Sol. Energy* 160 (2018) 336–343.
- [57] L. Fara, et al., Heterojunction tandem solar cells on Si-based metal oxides, *Energies* 16 (7) (2023) 3033.
- [58] L. Fara, et al., On numerical modelling and an experimental approach to heterojunction tandem solar cells based on Si and Cu<sub>2</sub>O/ZnO—results and perspectives, *Coatings* 14 (3) (2024) 244.
- [59] A. Amine, et al., Up-to-date literature review on Solar PV systems: technology progress, market status and R&D, *Journal of Cleaner Production* 362 (2022) 132339. ISSN 0959-6526.
- [60] M. Prashant, S.S. Chandel, A new integrated single-diode solar cell model for photovoltaic power prediction with experimental validation under real outdoor conditions, *Int. J. Energy Res.* 45 (1) (2021) 759–771.
- [61] W.S. Ebhota, P.Y. Tabakov, Influence of photovoltaic cell technologies and elevated temperature on photovoltaic system performance, *Ain Shams Eng. J.* 14 (7) (2023) 101984. ISSN 2090-4479.
- [62] P. Pandian, et al., A selective cross-tied array configuration technique for partial shaded solar PV system, *Electr. Eng.* (2024).